First Mapping Observations of Two Possible Cloud Collision Candidates IRAS 02459+6029 and 05363+3127 *

Bei Xin and Jun-Jie Wang

National Astronomical Observatories, Chinese Academy of Sciences, Beijing 100012, China
xinpei@hep.com.cn

Abstract The first mapping observations of the cold infrared sources IRAS 02459+6029 and 05363+3127 in the molecular lines ^{12}CO(1–0), ^{13}CO(1–0) and C^{18}O(1–0) were made using the 13.7 m millimeter wave telescope in Qinghai. Both the integrated intensity maps and position-velocity diagrams show that each has two components adjacent in both space and velocity which means possible cloud-cloud collisions in the two regions. The near-infrared color-color diagram from the 2MASS database reveals that the density of YSOs in the colliding site is much higher than in the surrounding regions. The results appear to indicate that star forming activities have taken place in the two regions due to the cloud-cloud collision. We conclude that both sources are cloud collision candidates.

Key words: stars: formation — ISM: clouds

1 INTRODUCTION

Collapse of molecular clouds in star forming regions could be triggered by self-gravity or some external perturbations (Evans 1991). Collapse through self-gravity occurs when the mass of the cloud is greater than the Jeans mass. Then the cloud fragments into filaments and clumps, and only dense clumps collapse to form stars (Klessen et al. 1998). However, the formation of stars through ionization-driven shocks, supernova shocks, stellar winds, and shocks due to cloud-cloud collisions is not well understood. Local density of molecular clouds will be increased and their system will be unstable due to interaction between the shocks and the clouds. Cloud-cloud collision has been thought as an effective mechanism to induce the shocks and the cloud instability. As the cloud collapses, a new generation of stars forms (Wang et al. 2004).

In a previous work, we selected a sample of IRAS sources from a large-scale molecular survey by Yang et al. (2002). We conducted a survey to all the IRAS sources and built up a sample of candidates of star forming regions triggered by molecular cloud collision. In this letter, we report some mapping observations toward two possible cloud-cloud collision candidates, IRAS 02459+6029 and 05363+3127, which were picked up from the above sample.

The cold infrared sources, IRAS 02459+6029, is associated with RAFGL 5084 in the molecular cloud complex W3/W4/W5. Its distance is about 4 kpc, its radius is above 0.8 pc and its mass is above 800 $M_\odot$ (Carpenter et al. 2000). The source IRAS 05363+3127 is associated with DG 069 at a distance of 0.65 kpc. This infrared source has rarely been observed.

2 OBSERVATIONS

The mapping observations of IRAS 02459+6029 and 05363+3127 in the molecular lines ^{12}CO(1–0), ^{13}CO(1–0) and C^{18}O(1–0) were made with the 13.7 m Millimeter Wave Telescope at the Qinghai Station

of Purple Mountain Observatory, CAS, in January 2007. A cooled mixer SIS receiver, with observing at 115 GHZ (^{12}CO) and at 110 GHz (^{13}CO and C^{18}O) was used. The main beam width is $54'' \times 54''$, and the pointing and tracking accuracy is better than $10''$. The AOS spectrometer has 1024 channels with a total band width of 145 MHz (^{12}CO) or 43 MHz (^{13}CO and C^{18}O), corresponding to a velocity resolution of 0.37 km s^{-1}(^{12}CO) or 0.11 km s^{-1}(^{13}CO and C^{18}O). The antenna efficiency is 0.50. All the spectra of the two sources were taken in the absolute-position-switching mode. These mapping observations were centered at (RA(2000)=02^{h}49^{m}47.6^s, Dec(2000)=60^{h}42^{m}07.26^s) for IRAS 02459+6029, and at (RA(2000)=05^{h}39^{m}35.84^s, Dec(2000)=31^{h}29^{m}12.16^s) for IRAS 05363+3127. The mapping grid spacing was $0.5'$, and the integration time was 1 minute at each position. The receiver noise temperature was 250 K during our observations, and typical rms was 0.20 K. The spectral line intensity T* $_A$ was calibrated with the ambient temperature and corrected for atmospheric absorption. The data were reduced with the software packages, CLASS (Continuum and Line Analysis Single-disc Software) and GREG (Grenoble Graphic) .

3 DATA PROCESSING AND RESULTS

Figure 1 shows the ^{12}CO, ^{13}CO and C^{18}O spectra centered on the IRAS 02459+6029 and 05363+3127 regions. The spectra of IRAS 02459+6029 have a double-peaked main line, with peaks at –41 and –36 km s $^{-1}$ in the local standard rest frame (LSR). The spectra at IRAS 05363+3127 position also show a double-peaked main line at –2 and 1.2 km s^{-1}. There are different interpretations of double-peaked profile in optically thick ^{12}CO lines, including self-absorption, outflow, infall, rotation and two clouds configuration, etc. The optically thin spectra in ^{13}CO and C^{18}O lines also show the same double peaks as in the ^{12}CO line, with the same LSR velocities. Comparing the spectral profile of ^{12}CO with those of ^{13}CO and C^{18}O, one can exclude the configuration of self-absorption, infall, outflow and rotation from our two observed sources (Zhou et al. 1993; Dobashi et al. 1993; Walsh et al. 2002). It seems that the two velocity components in the molecular lines of IRAS 02459+6029 and 05363+3127 originate in two separated clouds (Wang et al. 2004).
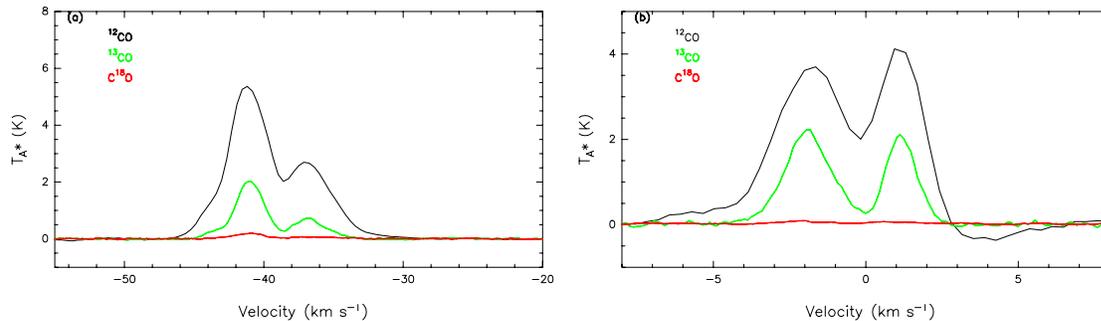
Fig. 1 (a) The spectra in the molecular lines ^{12}CO, ^{13}CO and C^{18}O of IRAS 02459+6029 show a double-peaked main line at –41 and –36 km s^{-1}. (b) The spectra of IRAS 05363+3127 have a double-peaked main line at –2 and 1.2 km s^{-1}.

In order to investigate possible kinematics and star forming activities of the cores in the two regions, we constructed the integrated intensity maps and the position-velocity diagrams. Now, the optically thick ^{12}CO line samples the emission from the envelope of the cloud and so is not good for studying the kinematics of the compact cores. Again, of the C^{18}O line, the signal-to-noise ratio in our observation is below 1.5, which is inadequate for our purpose. Thus we are left only with the maps in the ^{13}CO line for our investigation.

Figure 2(a) shows the integrated intensity map of IRAS 02459+6029 in the molecular line ^{13}CO(1–0). The observed positions are marked. The grey contours show the integrated intensities over the velocity range –43.6 to –38.4 km s^{-1}, the wedge indicates the intensity scale 4.5 to 15 K km s^{-1} (the 3σ value is 0.44 K km s^{-1}). The solid contours mark the integrated intensities over the velocity range –38.4 to –33 km s^{-1}, with contour values from 2.83 to 9.42 K km s^{-1} (the 3σ value is 0.33 K km s^{-1}). Both sets display levels 30%, 40%, 50%, 60%, 70%, 80%, 90% and 100% of the maximum intensity. The cutoff of
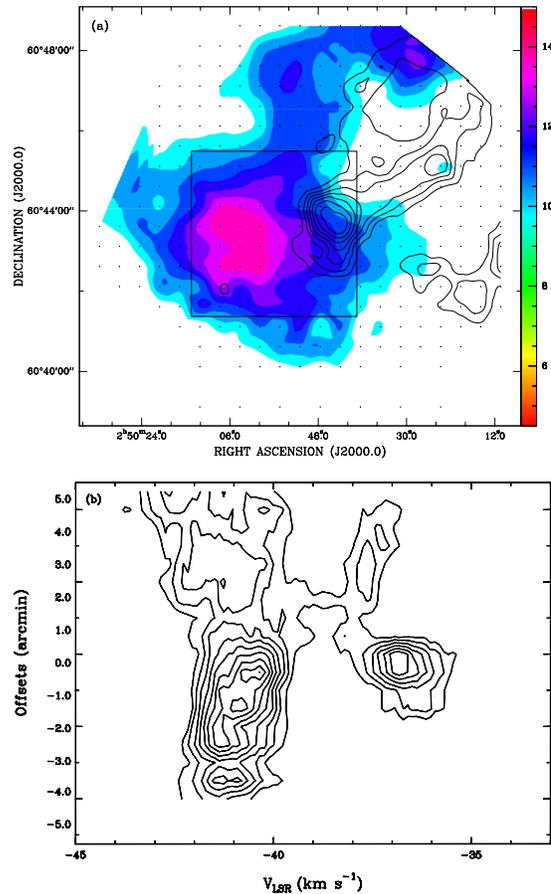
Fig. 2 (a) Integrated intensity map in the molecular line ^{13}CO(1–0) toward IRAS 02459+6029. The grey contours are integrated intensities over the velocity range –43.6 to –38.4 km s^{-1}, the wedge indicates the intensity scale from 4.5 to 15 K km s^{-1} (the 3σ value is 0.44 K km s^{-1}). The solid contours indicate the integrated intensities over the velocity from –38.4 to –33 km s^{-1}, and the contour values are from 2.83 to 9.42 K km s^{-1} (the 3σ value is 0.33 K km s^{-1}). The square marks the region of collision of the two clouds. (b) Position-velocity diagram of IRAS 02459+6029, with the contours increasing from 1.10 to 5.48 K, at steps of 0.55 K.

more than 20σ in the first contour filters out the diffuse emission of the molecular cloud and only picks out the compact region, which will be useful for the kinematical study of the core regions. There are two compact cores in Figure 2(a). The separation between the two cores is about 2$'$, corresponding to a linear separation of 0.002 kpc. It appears that the two clouds are spatially adjacent.

Figure 2(b) shows the position-velocity diagram in ^{13}CO(1–0) of the IRAS 02459+6029 region along the declination direction. The contours are from 1.10 K to 5.48 K in steps of 0.55 K (the 3σ value is 0.6 K). In Figure 2(b) the two velocity components centering at –41 and –36 km s^{-1}, respectively, correspond to the two components shown by the grey and solid contours of Figure 2(a). The two velocity components of IRAS 02459+6029 are adjacent.

The integrated intensity contour of ^{13}CO(1–0) line toward IRAS 05363+3127 is shown in Figure 3(a). The grey contours show the integrated intensities over the velocity range –3.34 to 0.33 km s^{-1}, and the contour values are from 1.76 to 5.85 K km s^{-1} in steps of 0.59 K km s^{-1} (the 3σ value is 0.36 K km s^{-1}). The black contours show the integrations from 0.33 to 2.41 km s^{-1}, the contour values are from 1.26 to 4.22 K km s^{-1} in steps of 0.42 K km s^{-1} (the 3σ value is 0.34 K km s^{-1}). The separation of the two cores is 1.5$'$, corresponding to 0.0003 kpc linear size. It seems that two clouds are adjacent in space.
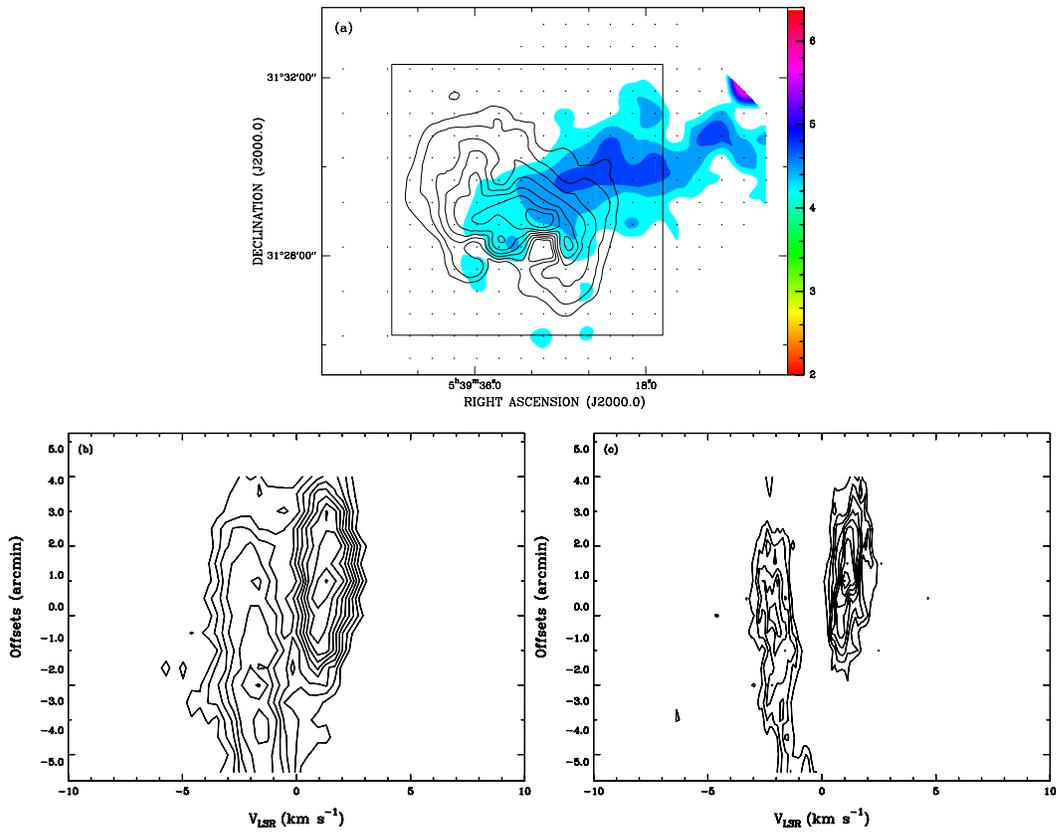
Fig. 3 (a) Integrated intensity map of IRAS 05363+3127 in ^{13}CO(1–0). The grey contours show the integrated intensities over the velocity range −3.34 to 0.33 km s^{-1}, the contour value increasing from 1.76 to 5.85 K km s^{-1} at steps of 0.59 K km s^{-1}, and the 3σ value is 0.36 K km s^{-1}. The solid contours are integrations from 0.33 to 2.41 km s^{-1}, with contour values from 1.26 to 4.22 K km s^{-1} in steps of 0.42 K km s^{-1}, the 3σ value being 0.34 K km s^{-1}. The square marks the colliding region of the two clouds, see Sect. 4 for more details. (b) Position-velocity diagram of IRAS 05363+3127 in ^{12}CO(1–0). The contour levels are from 0.66 K to 5.07 K in steps of 0.55 K (the 3σ value is 0.6 K). (c) Position-velocity diagram of IRAS 05363+3127 in ^{13}CO(1–0). The contour levels are from 0.62 K to 3.09 K in steps of 0.31 K (the 3σ value is 0.6 K).
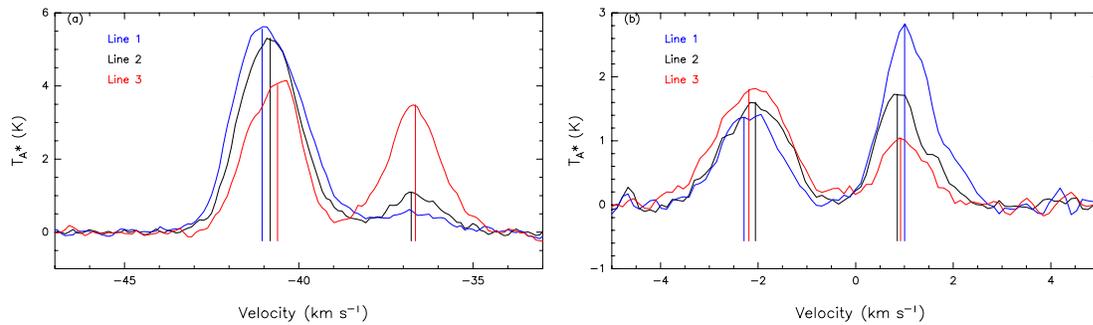
Fig. 4 (a) Spectra of the overlapping (colliding) and core regions of the clouds of IRAS 02459+6029. (b) Spectra of the overlapping (colliding) and core regions of the clouds of IRAS 05363+3127.

Figure 3(b) presents the position-velocity diagram in ^{12}CO(1–0) of the IRAS 05363+3127 region along the direction of right ascension. The two velocity components located at –2 and –1.4 km s^{-1} correspond to the grey and solid contours in Figure 3(a), respectively. The contours increase from 0.66 K to 5.07 K, at steps of 0.55 K (the 3σ value is 0.6 K). Obviously, the two velocity components are adjacent too.

The position-velocity diagram in the molecular line ^{13}CO(1–0) of the IRAS 05363+3127 region along the right ascension direction (Fig. 3(c)) shows two velocity components, with the contour levels from 0.62 K to 3.09 K at steps of 0.31 K (the 3σ value is 0.6 K). The diagram shows two separate velocity components, at the same positions as in Figure 3(b).

The overlapping regions and core regions of the two IRAS sources were examined in more details. We selected a number of points in the overlapping and the core regions of the two clouds, and picked out the ^{13}CO(1–0) molecular lines at those points. Figure 4(a) presents the spectra of IRAS 02459+6029. The left peak of line 1 is the average of the selected ^{13}CO(1–0) lines in the core region of cloud A. The peak is at –40.98 km s^{-1}, which is drawn in blue. Line 2 drawn in black, is the spectrum of the overlapping region between the two cores, and the two peaks are at –40.7 and –36.82 km s^{-1}. Moreover, the right peak of line 3 indicates the core region of cloud B, which peaks at –36.6 km s^{-1} and is drawn in red. The left peak of line 1 shows a blue shift with respect to line 2, indicating that cloud A is moving toward the overlapping region. The right peak of line 3 shows a red shift with respect to line 2, indicating that cloud B is moving away from the overlapping region. The two clouds are moving toward each other. We suggest that the two components in IRAS 02459+6029 are possibly interactive.

Figure 4(b) shows the spectrum of the molecular line ^{13}CO(1–0) of IRAS 05363+3127. The left peak of line 1 represents the average molecular lines selected from the core region of cloud A, it peaks at –2.16 km s^{-1}, and is drawn in blue. Line 2 (drawn in black) shows the spectrum of the overlapping region between the two cores. The two peaks are at –2.0 and 0.76 km s^{-1}. The right peak of line 3 (in red) represents the core region of cloud B, which is at 0.91 km s^{-1}. The left peak of line 1 presents a blue shift with respect to line 2, indicating that cloud A is moving toward the overlapping region. The right peak of line 3 shows a red shift with respect to line 2, indicating that cloud B is moving away from the overlapping region. Similar to the case of IRAS 02459+6029, the two clouds are moving toward each other, and we suggest that the two components in IRAS 05636+3127 are possibly interactive as well.

4 ANALYSIS AND DISCUSSION

The observations show that IRAS 02459+6029 and 05363+3127 each has two velocity components that originate in two different clouds. In each case, the two components are adjacent in space and velocity and are moving towards each other. Our results appear to satisfy the criterion of cloud-cloud collision (Vallee et al. 1990; Vallee et al. 1992; Vallee et al. 1993; Vallee 1995a,b), and there is probably a cloud-cloud collision in each of the two regions. Consider now the position-velocity diagrams of the two regions in the different lines. For IRAS 02459+6029, the two velocity components are adjacent in both the ^{12}CO(1–0) and ^{13}CO(1–0) lines. However, for IRAS 05363+3127, the velocity components are adjacent in ^{12}CO(1–0) and are separate in the optically thin ^{13}CO(1–0) line. It seems that the ^{12}CO line reflects the envelope while the ^{13}CO line reflects the inner regions. The position-velocity diagram indicates that the time scale of collision is longer, and the colliding region (the overlapping part) is deeper, in IRAS 02459+6029 than in IRAS 05363+3127. The collision in IRAS 05363+3127 could be just at the beginning phase.

According to the 2MASS data, there are some 92 near infrared sources in the $4' \times 4'$ region (Fig. 2(a)) around IRAS 02459+6029 and 166 in the $6' \times 6'$ region (Fig. 3(a)) around IRAS 05363+3127. These squares were chosen depending on the scale of the colliding regions in ^{12}CO(1–0) (not shown here). An error of about $1' \times 1'$ was also considered based on the beam size of the molecular line observations. Sources with J-H<0.6 and H-K<0.4 are possibly foreground stars, and so were excluded, leaving 40 sources around IRAS 02459+6029 and 18 sources around IRAS 05363+3127. We then obtained the color-color diagrams shown in Figure 5, in which the two dashed lines bracket reddened foreground or background main-sequence stars. All the sources to the right of the reddened vectors are possibly young stellar objects (Weintraub et al. 1996). The statistics of the density of the young stellar objects is as follows: there are about 2.5 sources per square arcmin in the colliding region of IRAS 02459+6029, and 0.84 sources per square arcmin in its surrounding area. For IRAS 05363+3127, the density is 0.5 sources per square arcmin in the colliding region and 0.33 sources per square arcmin in the surrounding area. The density of young stellar objects is much higher in the
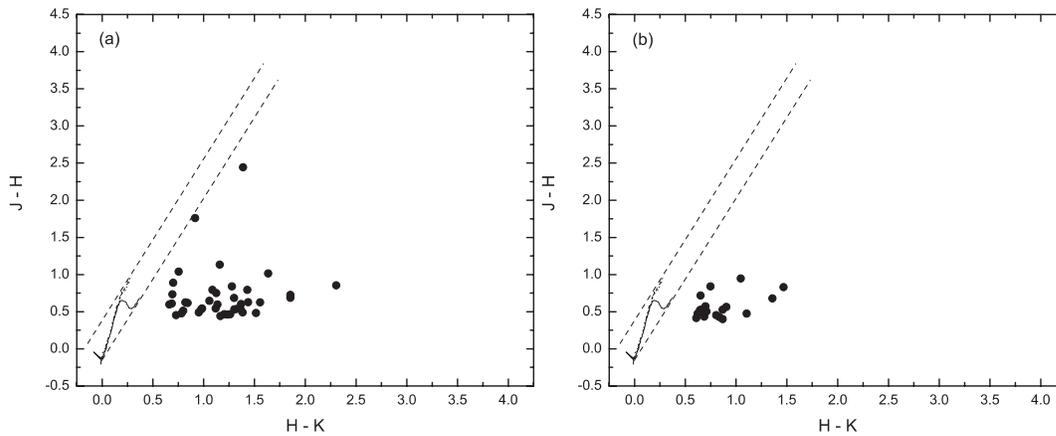
Fig. 5 (a) JHK color-color diagram for IRAS 02459+6029, for the selected sources in the $4' \times 4'$ square shown in Fig. 2(a). The dashed lines mark the interstellar reddening vectors. There are 40 possible young stellar objects to the right of the reddening line in the selected region. (b) JHK color-color diagram of IRAS 02459+6029 for selected sources in the $6' \times 6'$ square of Fig. 3(a). There are 18 young stellar objects in this region.

colliding regions than in the surrounding regions for both molecular clouds, indicating formation of stars in the former. Cloud-cloud collision is a possible efficient trigger of cloud collapse leading to star formation.

5 SUMMARY

The first mapping observation in three wavelengths, ^{12}CO(1–0), ^{13}CO(1–0) and C^{18}O(1–0) for IRAS 02459+6029 and 05363+3127 are presented. Both the integrated intensity maps and position-velocity diagrams show two clouds adjacent in space and velocity. Together with a study on the average molecular lines, we found that, for both IRAS 02459+6029 and 05363+3127, the two components are interactive, indicating possible cloud-cloud collision in the two regions. Many young stellar objects are detected in the colliding regions. Star formation is probably on-going in the colliding region of the two clouds, and could have been triggered by the cloud collision.

References

Dobashi K., Onishi T., Iwata T., 1993, AJ, 105, 1487
Evans Neal J., II, 1991, ASPC, 20, 45
John M. C., Mark H. H., Ronald L. S., 2000, AJ, 130, 381
Klessen R. S., Burkert A., Bate M. R., 1998, ApJ, 501, 205
Vallee J. P., Avery L. W., 1990, A&A, 233,553
Vallee J. P., de Bruyu A. G., 1992, ApJ, 393,674
Vallee J. P., Kompe C., 1993, AJ, 106,1561
Vallee J. P., 1995a, AJ, 109, 1724
Vallee J. P., 1995b, AJ, 110, 2256
Walsh W., Beck R., Thuma G. et al., 2002, A&A, 388, 7
Wang J.- J., Chen W.- P., Miller M. et al., 2004, ApJ, 614, 105
Weintraub D. A., Kastner J. H., 1996, AJ, 458, 670
Yang J., Jiang Z., Wang M. et al., 2002, AJ, 141,157
Zhou S., Evans N. J., II, Koempe C., Walmsley C. M., 1993, ApJ, 404, 232